Research Square

Preprints are preliminary reports that have not undergone peer review.
They should not be considered conclusive, used to inform clinical practice,
or referenced by the media as validated information.

Emulating interacting waveguide quantum electrodynamics with wire metamaterials

Eugene Koreshin (evgeniy.koreshin@metalab.ifmo.ru)
ITMO University https://orcid.org/0000-0002-7980-2174
Denis Sakhno
ITMO University https://orcid.org/0000-0003-0697-4765
Alexander Poddubny
Ioffe Institute, ITMO University
Pavel Belov
ITMO University https://orcid.org/0000-0002-5107-2763

Article

Keywords: analogue quantum simulations, waveguide quantum electrodynamics, electromagnetic wave, wire metamaterial

Posted Date: August 26th, 2021

DOI: https://doi.org/10.21203/rs.3.rs-827978/v1

License: This work is licensed under a Creative Commons Attribution 4.0 International License.
Read Full License

Emulating interacting waveguide quantum electrodynamics with wire metamaterials

Evgeniy A. Koreshin,[1,*] Denis I. Sakhno,[1] Alexander N. Poddubny,[2,1,†] and Pavel A. Belov[1]

[1] *ITMO University, St. Petersburg 197101, Russia*

[2] *Ioffe Institute, St. Petersburg 194021, Russia*

(Dated: August 19, 2021)

Abstract

Arrays of atoms coupled to photons, propagating in a waveguide, are now actively studied due to their prospects for generation and detection of quantum light. Quantum simulators based on waveguides with long-range couplings were also predicted to manifest unusual many-body quantum states. However, quantum tomography for large arrays with $N \gtrsim 20$ atoms remains elusive since it requires independent access to every atom. Here, we present a novel concept for analogue quantum simulations by mapping the setup of waveguide quantum electrodynamics to the classical problem of an electromagnetic wave, propagating in a wire metamaterial. By experimentally measuring the near electromagnetic field we emulate the localization arising from polariton-polariton interactions in the quantum problem. Our results demonstrate the potential of wire metamaterials to visualize quantum light-matter coupling in a table-top experiment and may be applied to emulate other exotic quantum effects, such as quantum chaos, and self-induced topological states.

* evgeniy.koreshin@metalab.ifmo.ru

† poddubny@coherent.ioffe.ru

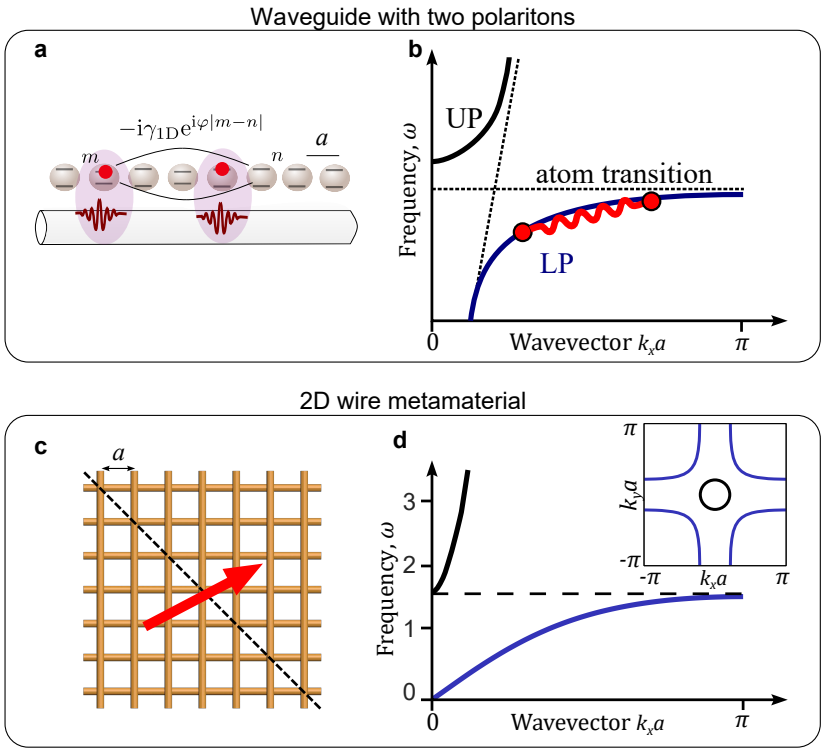

FIG. 1. **Schematics of quantum waveguide (top) and classical metamaterial (bottom) setup.** (a) Periodic array of atoms coupled to the waveguide with two propagating excitations. (b) Schematics of the polariton dispersion demonstrating avoided crossing of the light line with the atomic resonance at the frequency ω_0 and two interacting lower-branch polaritons (LP). (c) Two-dimensional metamaterial made of crossed wires with a propagating wave (red arrow) (d) Dispersion branch $\omega(k_x)$ in such a metamaterial plotted for $k_y = \pi/15a$. A typical isofrequency contour is shown in the inset.

I. INTRODUCTION

Waveguide quantum electrodynamics (WQED) is an emerging field of quantum optics studying interactions of atomic arrays, coupled to the waveguide, with the photons propagating inside the waveguide, as shown in Fig. 1a. The platforms for WQED include natural atoms, quantum defects, superconducting qubits[1–3]. The WQED setup can be harnessed to generate and detect quantum light [4], for slow light and quantum memory applications [5] and as a simulator of many-body quantum physics [6, 7]. The unique features of the WQED problem include strong non-Hermiticity due to the escape of photons into the waveguide, that can be both super- and sub- radiant and long-ranged waveguide-mediated interactions

between the atoms. Namely, contrary to the more conventional tight-binding setup where only neighboring atoms are coupled by tunneling, in the WQED an atom can emit a photon that will propagate for a long distance along the waveguide until being reabsorbed by another atom. This light-induced coupling is described by a very unusual non-Hermitian effective Hamiltonian [8, 9],

$$H = -\mathrm{i}\gamma_{1\mathrm{D}} \sum_{n,m=1}^{N} \sigma_n^\dagger \sigma_m \mathrm{e}^{\mathrm{i}\varphi|m-n|} \,, \tag{1}$$

where the energy is counted from the atomic resonance ω_0, σ are the atomic raising operators, $\sigma^2 \equiv 0$, $\varphi = \omega_0 d/c$ is the phase gained by light travelling the distance d between two neighboring atoms and $\gamma_{1\mathrm{D}} \equiv \Gamma_{1\mathrm{D}}/2$ is the radiative decay rate of single atom into the waveguide. The non-Hermiticity of the effective Hamiltonian reflects an open nature of the problem: excitations can decay radiatively into the waveguide. The single-excited eigenstates of the Hamiltonian Eq. (1) in the infinite array are quasiparticles, polaritons, with the wavevectors k and dispersion law $\varepsilon(k)$, determined by the equation [10–12] $\cos k = \cos\varphi - \mathrm{i}\gamma_{1\mathrm{D}} \sin\varphi/\varepsilon$ schematically illustrated in Fig. 1(b). The upper and lower polariton dispersion branches originate from the avoided crossing of the linear light dispersion (almost vertical dashed line) and the atomic resonance at $\varepsilon = 0$ (horizontal dashed line). The polaritons repel each other due to the photon blockade effect [13], i.e. a single two-level atom can not be excited twice. Such polariton-polariton interaction has recently been predicted to drive a number of interesting effects, including fermionization [14], formation of bound two-polariton pairs [15], interaction-induced localization [16] and topological states [17], quantum chaos [18] and many-body localization [19]. In a nutshell, the long-ranged interactions in Eq. (1) are manifested by peculiar wavefunctions of the many-body states. While single-particle eigenstates of Eq. (3) are just standing waves [3]

$$\psi_k \propto \sum_{n=1}^{N} \cos(kn + \alpha) \sigma_n^\dagger |0\rangle \,, \tag{2}$$

owing to the interactions there exist entangled two-particle wavefunctions that are irreducible to any simple combination of just one or two single-particle eigenstates of the finite array Eq. (2). Their Fourier transform contains a broad distribution of the wave vectors k [16, 18] which means that they are drastically modified by interactions. However, an observation of such rich interaction-induced physics described by the Hamiltonian Eq. (1)

is quite challenging already in the two-body case since it requires tomography of the excited subspaces of Hilbert space. This could be potentially done in the superconducting quantum processors, where each qubit can be accessed individually [20]. State-of-the-art results include probing of two-photon quantum walks in an array of 12 qubits with nearest-neighboring coupling [21], i.e. without the waveguide. Nevertheless, despite the tremendous recent progress in this field, including quantum supremacy for specific problems[20], tomography of many-body quantum states with large number of atoms $N \gtrsim 20$ remains a standing problem.

Here, we bypass the quantum tomography problem for the double-excited states in WQED by demonstrating that the two-polariton sector of the problem can be mapped to the classical electromagnetic problem with waves propagating in a two-dimensional wire metamaterial [22], shown Fig. 1c. The correspondence between the two-body one-dimensional quantum problem and a classical 2D problem is well known at least since the study of classical billiards [23] and different effects such a fractional Bloch oscillations [24], and interaction-induced topological edge states [25] have been successfully emulated classically. However, so far the studies have been limited to the tight-binding problems with nearest-neighbor coupling that are very different from the WQED problem Eq. (1). The quantum-classical correspondence for the polaritonic problem has remained elusive. In this work we build on the fact that the dispersion of electromagnetic waves in a wire metamaterial can be very similar to the polariton dispersion, compare Fig. 1d and Fig. 1b. The two coordinates x and y inside the metamaterial then correspond to the coordinates of first and second polariton in the quantum problem.

In order to test this approach here we emulate the effect of interaction-induced localization predicted in [16] with the two-polariton wavefunction of the form

$$\psi(x,y) = \psi_{\rm loc}(x) \cos\frac{\pi m y}{N} + (x \leftrightarrow y)\,, m = 1, 2 \ldots \tag{3}$$

where the wavefunction $\psi_{\rm loc}(x)$ is strongly spatially localized in the node (or antinode) of the standing wave $\cos \pi m y/N$. This wavefunction Eq. (3) describes the trapping of the first polariton by the standing wave formed by a second polariton and vice versa. Contrary to the conventional optical trap or Anderson localization, here the localization emerges solely from the interactions between the two polaritons and does not require any external traps or disorder. Our findings indicate high potential of the simple 2D metamaterial setup for

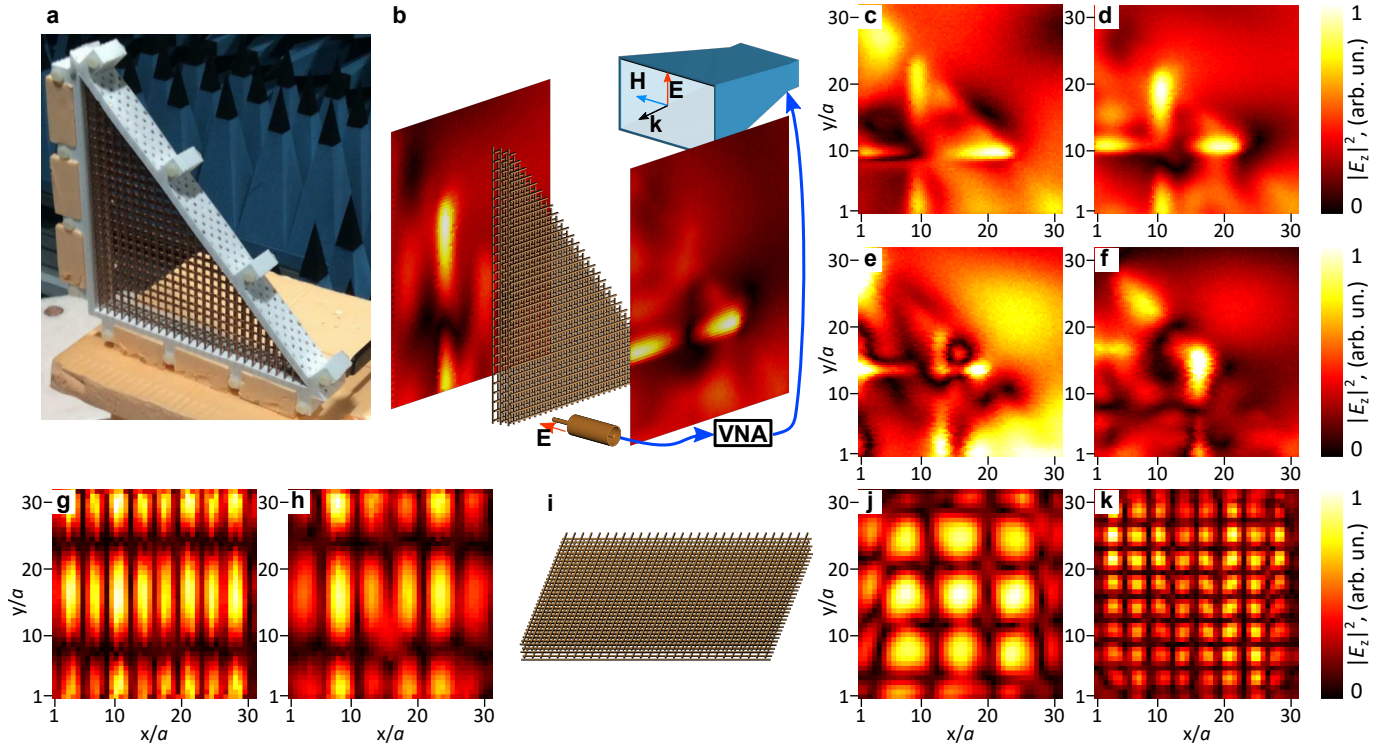

FIG. 2. Eigenstates of double wire medium. (a) Triangular experimental sample. (b) Schematic illustration of the experimental setup: horn antenna excited waves in the sample from far field, central core of coaxial cable was used to measure the near field distribution on both sides of the sample, both antennas were connected to Vector Network Analyzer. (c-f) Localized states obtained as the sum of fields at frequencies 1.08, 1.13, 1.33 and 1.53 GHz. (j) Square experimental sample in which localized states are absent, used as a reference. (g,h,j,k) Near field distributions at the frequencies 1.14, 1.32, 3.57 and 8.14 GHz

analogue modelling of complex many-body quantum physics in a cheap table-top experiment and will hopefully be useful for engineering and understanding of future quantum chips.

II. RESULTS

A. Quantum-classical correspondence

In order to demonstrate the similarity between quantum waveguide and wire metamaterial in radio frequency range we show the dependence of the frequency on a single component of the wave vector, while keeping the other components fixed. As an example, we present in

Fig. 1b the dispersion $\omega(k_x)$ calculated for $k_y a = \pi/15$. The low frequency mode (shown in blue) corresponded to hyperbolic isofrequency contour, high frequency curve corresponded to isotropic in-plane isofrequency contour. We consider a 2D wire metamaterial made of two sets of non-connected metallic wires extended along x and y axes. Parallel wires lie in the planes arranged with the period $a/2$, where a is the in-plane distance between the wires. Such structure supports two different mode types of the eigenmodes in the spectral range below the effective plasma frequency of the metamaterial [22]. We focus only on the wave propagation in the $x-y$ plane parallel to the wires and in the $k_x - k_y$ plane of reciprocal space. The perpendicular component of the wave vector k_z is assumed to be zero. One of the considered modes describes the waves propagating in the host medium without significant interaction with thin wires and has the electric field $\boldsymbol{E}$ polarized orthogonal to the wires plane, $\boldsymbol{E} \parallel z$. The corresponding isofrequency contour is just a circle (shown in black in the insert 1 d) with $k_x^2 + k_y^2 = (\omega/c)^2$. We are more interested in the second mode, where the isofrequency contour is represented by four hyperbola-like curves (shown in blue) with k_x and k_y greater than $\omega/c$and the electric field polarized in the $x-y$ plane [26]. The calculated dispersion of this mode as a function of k_x for the given value $k_y = \pi/(15a)$ is shown in Fig. 1d. Importantly, this dispersion branch has qualitatively the same shape as the lower polaritonic branch in the quantum setup, compare Fig. 1d and Fig. 1b..

The eigenmodes of a square metamaterial sample correspond to a pair of non-interacting polaritons. In order to introduce polariton-polariton interactions in the setup we make a diagonal cut in the metamaterial (dashed line in Fig. 1c) that effectively sets the boundary condition $\psi(x, y) = 0$ for $x = y$, describing the polariton-polariton repulsion (photon blockade). For wires in the free space, this boundary condition with open-ended wires corresponds to an extremum of electric field, and vanishing current and magnetic field. Such analogue simulation has allowed us to extract the two-polariton wavefunction from the near-field measurements in the metamaterial and emulate the polaritonic interactions in a simple classical setup.

B. Analogue simulation of self-induced localization

Our experimental setup is illustrated in Fig. 2a,b. In experiment, we consider just a lower triangle half of the diagonally cut square metamaterial structure, compare Fig. 1c

with Fig. 2a. We excite the structure from the far field by a close-to-plane wave, generated by the horn antenna positioned from the diagonal cut side of the sample. Next, we spatially scan the near electric field distribution by a local probe, as shown in Fig. 2b. The goal of such setup is to demonstrate that the localized electric field distribution, emulating interaction-induced localization of the two polaritons, arises from the intrinsic modes of the system and is not an artefact of the excitation. In addition to the triangular metamaterial structure, we also study a square sample as a reference, as shown in Fig. 2i. More details on sample preparation and measurement technique are given in Methods.

Our main experimental results are summarized by the near field scans in Fig. 2c–f that show characteristic localized features corresponding to the eigenmodes of the system. These scans correspond to the frequencies of 1081, 1130, 1326 and 1525 MHz (or normalized frequencies $\omega a/c = 0.128$, 0.135, 0.158 and 0.182). For comparison, we show in Fig. 2g,h,j,k the near field scans of the eigenmodes of a square sample. These eigenmodes are just the usual Fabry-Pérot modes, standing waves localized all over the structure and does not manifesting any localization. These results are in perfect qualitative agreement with the ansatz of the quantum theory Eq. (3). While the two-polariton states are delocalized without the interactions, the electric field in the triangular sample is localized transverse to the vertical wire and distributed along its length or it is localized transverse to the horizontal wire and distributed along its lengths, mimicking the interaction-induced localization of the two polaritons.

In order to further support this quantum-classical correspondence we have analyzed the localized electric field distribution for a particular localized mode shown in Fig. 2e in more detail. Namely, we have performed the Fourier analysis and also compared the experimental results with the full-wave electromagnetic simulations and the rigorous calculation of the corresponding quantum-mechanical problem. The results are summarized in Fig. 3. Figure 3a shows the same electric field distribution as in Fig. 2e but obtained with the source inside the sample (see Methods) along with its mirror reflection with respect to the triangle diagonal. The goal of the mirror reflection was to account for the bosonic symmetry of the two-polariton wave function, $\psi(x, y) = \psi(y, x)$. Figure 3b shows the same picture, but calculated numerically. It is in good agreement with the experimental result. The main difference is a broadening of the features of the experimental profile which is due to the finite resolution of our near field scanning setup. Also, the measured field distribution can

be potentially contributed by several modes. Finally, Fig. 3c illustrates the two-polariton wave function obtained by solving the Schrödinger equation [9, 16]

$$H_{mn'}\Psi_{n'n} + \Psi_{mm'}H_{m'n} - 2\delta_{mn}H_{mm'}\Psi_{n'm} = 2\varepsilon\Psi_{mn}\,. \tag{4}$$

Here, the indices $m, n, m', n' = 1 \ldots N$ label the atoms in the array, we assume summation over the dummy indices m', n' and 2ε is the energy of the two-polariton state. The Hamiltonian matrix elements are given by $H_{mn} = -\mathrm{i}\gamma_{1\mathrm{D}}\exp(\mathrm{i}\varphi|m-n|)$ as follows from Eq. (1). The phase φ in the quantum-mechanical calculation was equal to 0.15π, corresponding to the phase $\omega a/c$ in the experimental sample. The calculated two-polariton wavefunction in Fig. 3c well matches the measured near field scans as well as the results of the full-wave simulation.

More insight in the near field distributions is provided by their Fourier transforms, shown in the lower three panels of Fig. 3. All three Fourier transforms have qualitatively the same structure. First, they are concentrated along the hyperbolic isofrequency contours of the infinite structure, shown by red dotted curves in Fig. 3(e,f). Second, they are not localized in the reciprocal space but are distrubuted along the whole contour. Such reciprocal space delocalization is a direct counterpart of the localization of electric field and two-polariton wave function in the real space and well agrees with our earlier theoretical predictions in Refs. [16, 18].

We have also calculated numerically the near field distributions of other localized eigenmodes from Fig. 2c–f. In numerical simulations the same states exist at the frequencies of 1027, 1059, 1161 and 1268 MHz, respectively (or normalized $\omega a/c = 0.123$, 0.126, 0.139 and 0.151) and well agree with the experimental results, see the Supplementary Fig.**??**. The consistent agreement between the observed and calculated real- and reciprocal space patterns provides a solid basis that the observed localized electromagnetic distributions indeed emulate the waveguide quantum-electrodynamical problem where two polaritons interact and localize each other in space.

III. DISCUSSION

Waveguide quantum electrodynamics is a recently emerged and rapidly developing field of quantum optics, that promises many fundamental applications for future quantum technolo-

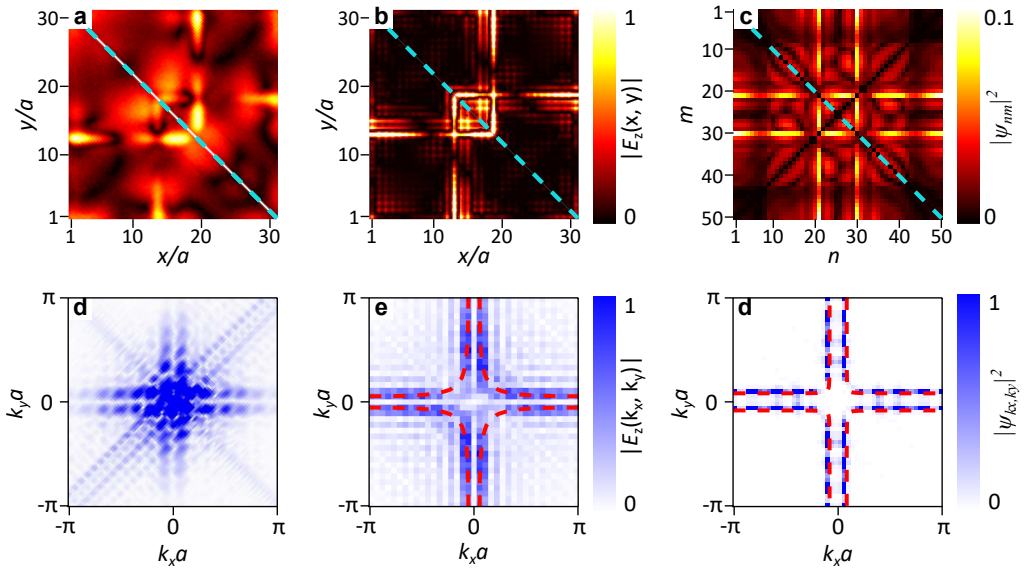

FIG. 3. **Real (top) and reciprocal spaces of localized states.** (a) Experimentally obtained electric field profile in double wire medium. (b) The same mode obtained numerically. (c) Strongly spatially localized two-wavefunction, calculated for the quantum problem. (d-f) Fourier spectra obtained by performing Fast Fourier Transform (FFT) from the real-space distribution. Dispersion in wire metamaterial is shown by the red dotted line in (e).

gies. Many intriguing effects known for interacting quantum systems, for example many-body localization [19, 27], have been predicted theoretically, but not observed yet in the waveguide setup. The reason is that quantum experiments are quite sophisticated, operating at cryogenic temperatures and requiring costly equipment. Even theoretical simulations of highly excited quantum states easily take several days [20, 28]. This makes analogue simulators based on wire metamaterials, such as the one proposed in our work, a simple platform for fast and cheap tests of novel ideas and visualization of fundamental quantum mechanical effects. One of the future avenues of research could involve studying larger samples to emulate self-induced topological states [17], where one of the polaritons creates a topologically nontrivial potential, trapping the second polariton at the edge of the structure. Our results can also be straightforwardly generalized to emulate a higher number of quantum excitations. Three-dimensional interlaced wire arrays [29] could mimic three interacting polaritons. Even higher number of quantum states could be implemented by judiciously engineering the coupling between electromagnetic elements. For example, Anderson localization in spaces with dimensionality larger than three has been recently successfully emulated in photonic

lattices [30]. Thus, we believe that theory and experiment for a few-body quantum problem and a classical electromagnetic metamaterial problem can stimulate each other and advance fundamental research and practical applications in both these fields.

Author contributions. AP and PB conceived the idea and supervised the project. EK made the sample and performed the experiment, EK, AP and DS performed the numerical calculations. All authors contributed to discussion of the results and writing the manuscript.

ACKNOWLEDGEMENTS

We are grateful to A.A. Bogdanov and M.A. Gorlach for useful discussions.

METHODS

A. Experimental methods

Sample fabrication. The sample was manufactured from individual wires with the lengths varying from 5.7 to 171 mm (from a to $30a$ with step a) and the diameter of 1.25 mm. It contained 6 layers with 30 wires in each layer, that were consistently oriented along x or y axes. The plastic holder needed to fixed the wires has been produced on 3D printer with ABS plastic, having the permittivity of about 2.4. We have also used a rectangular sample as a reference where all the wires had the same length $30a$.

Excitation. A rectangular sample, used as a reference, has been excited by a near field source. The isofrequency contours of double wire medium lie outside the vacuum dispersion and the conservation law for the component of the wave vector, tangential to the boundary, can not be satisfied. Thus, direct excitation of square sample from the far field has not been possible.

The field distribution in the reciprocal space has been obtained by measuring both the amplitude and the phase of the near field of the sample and performing the Fast Fourier Transform (FFT). In order to excite the wide range of wave vectors in the structure, we have used the generally accepted method of near field coupling with the electrically small source with a suitable polarization.

Near field measurements. An electric field probe, used to obtain the near-field distribution on both sides of the sample, has been realized as an electrically small monopole

antenna, represented by central core of coaxial cable. This type of antenna measures the component of the electric field along its core. We have ensured that the electromagnetic field source and the probe have not been coupled directly due to their orthogonal polarization. However, the probe was unbalanced, causing some part of the current to flow from the outer shell to the inner core. This has lead to the appearance of an additional low amplitude signal in the near field distribution, resulting in a background contribution to the near field. This contribution decreased the signal-to-noise ratio but has not affected the observation of the localized modes.

Both antennas have been connected to the vector network analyzer R&S ZVB20 (VNA) that has measured the transmission coefficient (S_{21}) proportional to the electric field amplitude near the probe and depending on the probe spatial position. The receiver has been moved by a 3D scanner in $x-y$ planes near the sides of the sample. The spatial step of the probe was equal to 1.9 mm that was three times smaller than the structure period.

In the ideal situation it would be desirable to measure the near field in the volume of the sample, between the sets of the wires. However, in our experimental setup this was hard to achieve because of the finite size of the probe. Moreover, when the probe is inserted inside the metamaterial it acts as a defect of the structure and modifies its electromagnetic properties. This effect has been already discussed in [31]. Thus, non-perturbative measurement of the field inside is quite challenging. In order to overcome this problem we have compared the field in the volume of the structure (between the planes of the wires) with the sum of the near fields for the two sides of the sample obtained numerically as an eigenmode of the structure in CST Microwave Studio solver. Our calculation indicates that the results obtained in such indirect way from the surface field distributions and directly from inside the sample are close to each other, as demonstrated by the Supplementary Fig.**??**. This agreement has allowed us to simplify the measurement procedure. In experiment, we have measured the near electric field from both sides of the sample and added the absolute values from the top and bottom sides together. This result serves as a satisfactory approximation equal to the field distribution inside the sample. The measured fields from the two sides are also illustrated in Fig. 2b.

B. Numerical simulations

Numerical simulations were performed in the Eigenmode solver of the CST Microwave Studio commercial software package. The simulated triangle had exactly the same geometrical dimensions as the experimental sample: 30 by 30 wires along sides, spacing between wires in plane was $a = 5.7$ mm, between planes $a/2$. In order to accelerate the calculations we have chosen the square cross-section of the wires 1.25×1.25 mm instead of the circular cross section. Our numerical model has also included dielectric holder with the permittivity of 2.4. We have used the perfect electric conductor (PEC) boundary condition with the additional spacing of $5a$ between the model and the boundary. Since the boundary has been placed relatively far from the sample, it is safe to assume that additional capacitance is negligible and has not influenced the accuracy of the calculation of the field distribution. The calculated eigenfrequencies are slightly smaller than those in experiment due to this type of boundary conditions.

[1] D. Roy, C. M. Wilson, and O. Firstenberg, "*Colloquium:* strongly interacting photons in one-dimensional continuum," Rev. Mod. Phys. **89**, 021001 (2017).

[2] D. E. Chang, J. S. Douglas, A. González-Tudela, C.-L. Hung, and H. J. Kimble, "*Colloquium:* quantum matter built from nanoscopic lattices of atoms and photons," Rev. Mod. Phys. **90**, 031002 (2018).

[3] A. S. Sheremet, M. I. Petrov, I. V. Iorsh, A. V. Poshakinskiy, and A. N. Poddubny, "Waveguide quantum electrodynamics: collective radiance and photon-photon correlations," (2021), arXiv:2103.06824 [quant-ph].

[4] A. S. Prasad, J. Hinney, S. Mahmoodian, K. Hammerer, S. Rind, P. Schneeweiss, A. S. Sørensen, J. Volz, and A. Rauschenbeutel, "Correlating photons using the collective nonlinear response of atoms weakly coupled to an optical mode," Nature Photonics **14**, 719 (2020).

[5] N. V. Corzo, J. Raskop, A. Chandra, A. S. Sheremet, B. Gouraud, and J. Laurat, "Waveguide-coupled single collective excitation of atomic arrays," Nature **566**, 359–362 (2019).

[6] S. J. Masson, I. Ferrier-Barbut, L. A. Orozco, A. Browaeys, and A. Asenjo-Garcia, "Many-body signatures of collective decay in atomic chains," Phys. Rev. Lett. **125**, 263601 (2020).

[7] A. González-Tudela, C.-L. Hung, D. E. Chang, J. I. Cirac, and H. J. Kimble, "Subwavelength vacuum lattices and atom–atom interactions in two-dimensional photonic crystals," Nature Photonics **9**, 320–325 (2015).

[8] T. Caneva, M. T. Manzoni, T. Shi, J. S. Douglas, J. I. Cirac, and D. E. Chang, "Quantum dynamics of propagating photons with strong interactions: a generalized input–output formalism," New J. Phys. **17**, 113001 (2015).

[9] Y. Ke, A. V. Poshakinskiy, C. Lee, Y. S. Kivshar, and A. N. Poddubny, "Inelastic scattering of photon pairs in qubit arrays with subradiant states," Phys. Rev. Lett. **123**, 253601 (2019).

[10] G. D. Mahan and G. Obermair, "Polaritons at surfaces," Phys. Rev. **183**, 834–841 (1969).

[11] E. L. Ivchenko, "Excitonic polaritons in periodic quantum-well structures," Sov. Phys. Sol. State **33**, 1344–1346 (1991).

[12] A. Albrecht, L. Henriet, A. Asenjo-Garcia, P. B. Dieterle, O. Painter, and D. E. Chang, "Subradiant states of quantum bits coupled to a one-dimensional waveguide," New J. Phys. **21**, 025003 (2019).

[13] K. M. Birnbaum, A. Boca, R. Miller, A. D. Boozer, T. E. Northup, and H. J. Kimble, "Photon blockade in an optical cavity with one trapped atom," Nature (London) **436**, 87–90 (2005).

[14] Y.-X. Zhang and K. Mølmer, "Theory of subradiant states of a one-dimensional two-level atom chain," Phys. Rev. Lett. **122**, 203605 (2019).

[15] Y.-X. Zhang, C. Yu, and K. Mølmer, "Subradiant bound dimer excited states of emitter chains coupled to a one dimensional waveguide," Phys. Rev. Research **2**, 013173 (2020).

[16] J. Zhong, N. A. Olekhno, Y. Ke, A. V. Poshakinskiy, C. Lee, Y. S. Kivshar, and A. N. Poddubny, "Photon-mediated localization in two-level qubit arrays," Phys. Rev. Lett. **124**, 093604 (2020).

[17] A. V. Poshakinskiy, J. Zhong, Y. Ke, N. A. Olekhno, C. Lee, Y. S. Kivshar, and A. N. Poddubny, "Quantum hall phases emerging from atom–photon interactions," npj Quantum Information **7**, 34 (2021).

[18] A. V. Poshakinskiy, J. Zhong, and A. N. Poddubny, "Quantum chaos driven by long-range waveguide-mediated interactions," Phys. Rev. Lett. **126**, 203602 (2021).

[19] N. Fayard, L. Henriet, A. Asenjo-Garcia, and D. Chang, "Many-body localization in waveguide QED," (2021), arXiv:2101.01645 [quant-ph].

[20] F. Arute *et al.*, "Quantum supremacy using a programmable superconducting processor," Nature **574**, 505–510 (2019).

[21] Z. Yan, Y.-R. Zhang, M. Gong, Y. Wu, Y. Zheng, S. Li, C. Wang, F. Liang, J. Lin, Y. Xu, C. Guo, L. Sun, C.-Z. Peng, K. Xia, H. Deng, H. Rong, J. Q. You, F. Nori, H. Fan, X. Zhu, and J.-W. Pan, "Strongly correlated quantum walks with a 12-qubit superconducting processor," Science **364**, 753–756 (2019).

[22] C. Simovski and P. Belov, "Low-frequency spatial dispersion in wire media," Physical Review E **70**, 046616 (2004).

[23] J. B. McGuire, "Study of exactly soluble one-dimensional n-body problems," J. Math. Phys. **5**, 622–636 (1964).

[24] G. Corrielli, A. Crespi, G. Della Valle, S. Longhi, and R. Osellame, "Fractional Bloch oscillations in photonic lattices," Nature Communications **4**, 1555 (2013), 10.1038/ncomms2578, arXiv:1303.1958 [quant-ph].

[25] N. A. Olekhno, E. I. Kretov, A. A. Stepanenko, P. A. Ivanova, V. V. Yaroshenko, E. M. Puhtina, D. S. Filonov, B. Cappello, L. Matekovits, and M. A. Gorlach, "Topological edge states of interacting photon pairs emulated in a topolectrical circuit," Nature Communications **11**, 1436 (2020).

[26] M. G. Silveirinha, "Broadband negative refraction with a crossed wire mesh," Physical Review B **79**, 153109 (2009).

[27] A. Polkovnikov, K. Sengupta, A. Silva, and M. Vengalattore, "Colloquium: Nonequilibrium dynamics of closed interacting quantum systems," Rev. Mod. Phys. **83**, 863–883 (2011).

[28] G. P. Fedorov, S. V. Remizov, D. S. Shapiro, W. V. Pogosov, E. Egorova, I. Tsitsilin, M. Andronik, A. A. Dobronosova, I. A. Rodionov, O. V. Astafiev, and A. V. Ustinov, "Photon transport in a bose-hubbard chain of superconducting artificial atoms," Phys. Rev. Lett. **126**, 180503 (2021).

[29] H. Latioui and M. G. Silveirinha, "Light tunneling anomaly in interlaced metallic wire meshes," Phys. Rev. B **96**, 195132 (2017).

[30] L. J. Maczewsky, K. Wang, A. A. Dovgiy, A. E. Miroshnichenko, A. Moroz, M. Ehrhardt, M. Heinrich, D. N. Christodoulides, A. Szameit, and A. A. Sukhorukov, "Synthesizing multidimensional excitation dynamics and localization transition in one-dimensional lattices," Nature Photonics **14**, 76–81 (2019).

[31] S. V. Silva, T. A. Morgado, and M. G. Silveirinha, "Comb-like modal dispersion diagram in a double-wire medium slab," IEEE Transactions on Antennas and Propagation **68**, 1755–1760 (2019).

Supplementary Files

This is a list of supplementary files associated with this preprint. Click to download.

- Supplementary.pdf